Geoderma 448 (2024) 116951

Contents lists available at ScienceDirect

Geoderma

journal homepage: www.elsevier.com/locate/geoderma

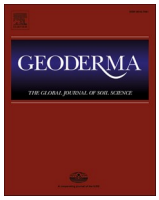

An adiabatic boundary condition with cylindrical perfect conductors for improved approximations from heat-pulse measurement near the soil-atmosphere interface

Wei Peng [a], Yili Lu [b,*], Tusheng Ren [b], Robert Horton [c]

[a] School of Geographical Sciences, Hebei Normal University, Shijiazhuang, Hebei 050024, China
[b] College of Land Science and Technology, China Agricultural University, Beijing 100193, China
[c] Department of Agronomy, Iowa State University, Ames, IA 50011, United States

ARTICLE INFO

Handling Editor: L. Morgan Cristine

Keywords:
Soil-atmosphere interface
Temperature
Heat pulse
Soil thermal property

ABSTRACT

The cylindrical-perfect-conductors (CPC) theory, which assumes an infinite and homogeneous soil medium, can be used to analyze heat pulse (HP) measurements to estimate soil thermal property values. However, when a HP sensor is positioned near the soil surface, the CPC theory is not valid because of the change in media properties at the soil-atmosphere interface. In this study, a CPC solution considering an adiabatic boundary condition (CPC-ABC) is presented to account for the soil-atmosphere interface effect. Compared with the results from numerical simulations, the CPC-ABC solution gave more accurate soil temperature values at the sensing probe than did a CPC model. When a HP sensor was positioned horizontally at a depth of 1 mm below a sand soil surface, the relative errors (*RE*) of CPC estimated thermal property values were as large as 52%, while the *RE* values based on the CPC-ABC solution were about 8%. Results from numerical simulations and laboratory experiments both showed that the CPC model worked well for horizontally positioned HP sensors with probe lengths of 70-mm at burial depths greater than 15 mm. Soil-atmosphere interface effect was largely dependent on HP sensor dimensions and measurement volumes. Overall, the extended CPC-ABC theory provided accurate soil thermal property estimates by considering the effects of finite probe properties and the presence of the soil-atmosphere interface.

1. Introduction

Soil thermal properties affect heat and water transfer in soils as well as energy partitioning at the ground surface. Accurate thermal property determinations of near-surface soil layers are vital for the study of coupled heat and water processes (Zhang et al., 2012, 2014; Liu et al., 2013). The heat-pulse (HP) method has been used extensively to measure soil thermal property values both in field and laboratory studies (He et al., 2018). The infinite line source (ILS) and cylindrical-perfect-conductor (CPC) theories, which are developed on the assumption of a homogeneous and infinite soil medium, are often applied to estimate soil thermal property values from the HP signals, i.e., temperature-by-time curves (Knight et al., 2012; Kamai et al., 2015; Peng et al., 2021; Kluitenberg et al., 2021). By placing a HP sensor near the soil-atmosphere interface, it can be used to monitor soil–water evaporation rates (Heitman et al., 2008; Xiao et al., 2014). However, when a HP sensor is positioned very close to the soil surface, there is a large contrast between soil and air thermal property values, and the effect of the soil-atmosphere interface on HP measurements should be considered (Philip and Kluitenberg, 1999; Liu et al., 2013; Peng et al., 2022). Thus, it is important to evaluate the performance of the ILS and CPC theories when HP measurements are made near the soil-atmosphere interface.

Philip and Kluitenberg (1999) proposed an approximate solution for an instantaneous heating scheme to estimate soil thermal property values from HP measurements near the soil-atmosphere interface. Neglecting soil-atmosphere interface effect on the HP measurements led to 50% errors in soil thermal property estimations (Philip and Kluitenberg, 1999; Xiao et al. 2015). Assuming the soil-atmosphere interface as an adiabatic boundary condition (ABC), Liu et al. (2013) extended the solution proposed by Philip and Kluitenberg (1999) by using a pulsed heat source. When measurements from a HP sensor that was installed horizontally at a 3-mm depth were analyzed with the Liu et al. (2013)

* Corresponding author.
E-mail address: luyili@cau.edu.cn (Y. Lu).

https://doi.org/10.1016/j.geoderma.2024.116951
Received 7 January 2024; Received in revised form 17 April 2024; Accepted 23 June 2024
Available online 14 July 2024

solution, the errors in thermal diffusivity (κ) and heat capacity (C) estimates were only about 5% (Liu et al., 2013). But Liu et al. (2013) solution ignored the finite probe properties such as radius (a) and probe thermal properties. Knight et al. (2012) proposed a CPC theory with a semi-analytical solution to account for the finite probe radius and probe heat capacity (C_p) when estimating soil thermal property values. Their analysis indicated that a and C_p could significantly impact HP temperature-by-time curves, especially on dry soils. Kamai et al. (2015) and Peng et al. (2019) used the CPC theory to obtain accurate estimates of soil thermal property values in laboratory conditions. There exists a need to account for soil-atmosphere interface effect within a CPC model to solve for soil thermal property values when HP sensors are positioned at shallow soil depths.

The objective of this study is to extend the CPC model to account for the soil-atmosphere interface effect when applied to HP sensor measurements made in near-surface soils. Numerical simulations with COMSOL and laboratory experiments are performed to evaluate soil-atmosphere interface effect on HP measurements and on the accuracy of the new CPC-ABC model to estimate soil thermal property values.

2. Materials and methods

2.1. Model development

According to Fig. 1, the HP sensor consists of a temperature (S) probe and a heater (H) probe mounted in parallel. The heater probe provides the pulsed heat source, and the temperature probe measures the soil temperature with time some distance away from the H probe. Campbell et al. (1991) first proposed the use of a heat pulse method to calculate soil specific heat values, and they reported that the maximum measurement boundary of a HP probe was approximately 2.37 times the probe spacing (r). Thus, the effect of the soil-atmosphere interface on HP measurements should be considered when a HP probe is positioned near the interface with the burial depth (h) $\leq 2.37r$, because the HP sensing range includes a soil region and an air region (Fig. 1), which embrace different thermal property values and heat transfer characteristics (Carslaw and Jaeger, 1959; Liu et al., 2013).

Knight et al. (2012) introduced the CPC theory with a semi-analytical solution that accounted for probe a and C_p when making soil thermal property estimates (Peng et al. 2021). For the case of continuous heating, the general solution in the Laplace transform domain of the temperature rise of the probe S at a known distance from the centerline of the probe H is,

$$\widehat{T}_0(p) = \widehat{v}_f(p, a_H, \beta_1)\widehat{v}_f(p, a_S, \beta_2)\frac{q' K_0(\mu r_0)}{2\pi\lambda p} \tag{1}$$

$$\begin{cases} \widehat{v}_f(p, a_H, \beta_1) = \dfrac{1}{\mu a_H[K_1(\mu a_H) + (\mu a_H \beta_1/2)K_0(\mu a_H)]} \\ \widehat{v}_f(p, a_S, \beta_2) = \dfrac{1}{\mu a_S[K_1(\mu a_S) + (\mu a_S \beta_2/2)K_0(\mu a_S)]} \end{cases} \tag{2}$$

where $\widehat{T}_0(p)$ is the Laplace transform of $T(t)$, i.e., the temperature data from the sensing probe; p is the Laplace transform parameter; a_H and a_S are the radii of the heater and temperature probes, respectively; $\beta_1 = C_{p1}/C$ and $\beta_2 = C_{p2}/C$, where C_{p1} and C_{p2} are the heat capacity of the heater and temperature probes, respectively; $K_z(g)$ denotes the modified Bessel function of the second kind of order z and argument g; $\mu = \sqrt{p/\kappa}$; The $\widehat{v}_f = (p, a_H, \beta_1)$ and $\widehat{v}_f = (p, a_S, \beta_2)$ are the corresponding transfer functions for the heater and temperature probes; q' is the heat input per unit length and unit time (W m^{-1}); r_0 is the distance between H and S; λ and κ are soil thermal conductivity (W m^{-1} K^{-1}) and thermal diffusivity (10^{-7} m^2 s^{-1}), respectively.

The presence of the soil-atmosphere interface was considered in ILS solution by Liu et al. (2013), which simplified the complex physical boundary conditions at the soil-atmosphere interface by approximating the soil-atmosphere interface as an ABC. Similarly, we adopted the methodologies reported by Liu et al. (2013) to derive the CPC-ABC model. The method of images assumed that ABC was equivalent to the presence of another heat source in the atmosphere (Carslaw and Jaeger, 1959). Based on the method of images, the two-dimensional composite soil-atmosphere system is depicted in Fig. 1b, where the heating strength of heater probe (H_1) in the atmosphere is as same as the probe H in the soil. The Laplace transform expression of the temperature rise at time t of probe S located in the soil caused by the heating from probe H_1 in the atmosphere is $\widehat{T}_1(p)$,

$$\widehat{T}_1(p) = \widehat{v}_f(p, a_H, \beta_1)\widehat{v}_f(p, a_S, \beta_2)\frac{q' K_0(\mu r_1)}{2\pi\lambda p} \tag{3}$$

$$r_1 = \sqrt{r^2 + 4h^2} \tag{4}$$

where r_1 is the distance between H_1 and S; h is the burial depth of a HP sensor.

In this case, a Laplace transform expression of the temperature rise at the temperature probe $\widehat{T}(p)$ is a superposition of $\widehat{T}_0(p)$ and $\widehat{T}_1(p)$ in

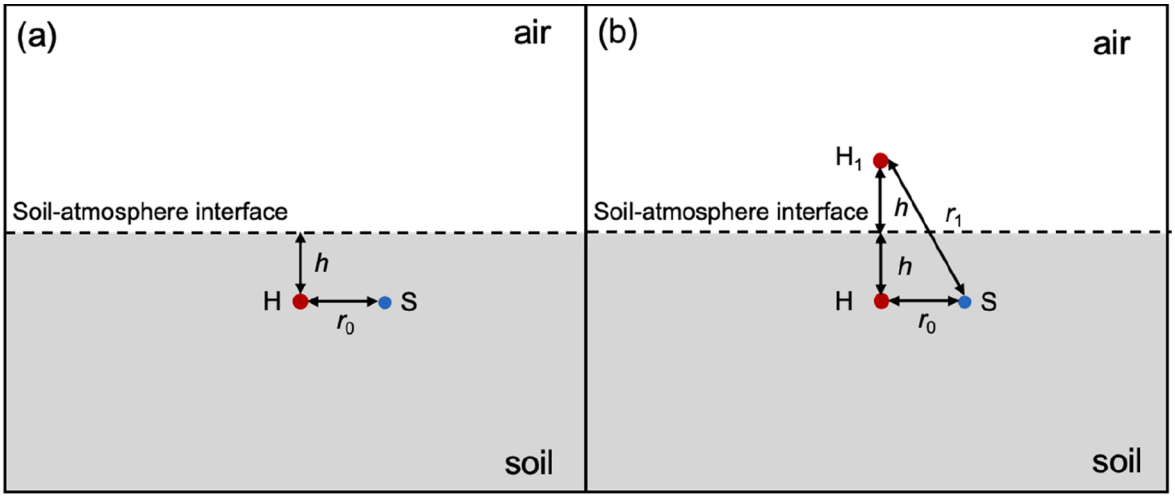

Fig. 1. Schematic diagram of (a) the two-dimensional scenario used in COMSOL simulations and (b) the counterpart mirror image scenario. H and H_1 represent heater probe positions in soil and in air, respectively; S represents the temperature probe; h is the distance between a heater probe and the soil-atmosphere interface; r_0 is the probe spacing between H and S; r_1 is the distance between H_1 and S.

space,

$$\widehat{T}(p) = \widehat{v}_f(p, a_H, \beta_1)\widehat{v}_f(p, a_S, \beta_2)\frac{q'}{2\pi\lambda p}[K_0(\mu r_0) + K_0(\mu r_1)] \quad (5)$$

The Laplace domain solution, Eq. (5), can be numerically inverted using the algorithm of Stehfest (1970a, 1970b) to solve for $T(t)$ and $T(t - t_0)$ for the case of a pulsed heating scheme,

$$T^P(t) = \begin{cases} T(t); 0 < t \leqslant t_0 \\ T(t) - T(t - t_0); t > t_0 \end{cases} \quad (6)$$

where $T^P(t)$ is the temperature data from the probe S under a pulsed heating scheme. Equations (1) to (6) represent the semi-analytical CPC-ABC solution for the case where the HP sensor is horizontally positioned near the soil-atmosphere interface ($h \leq 2.37r$).

2.2. Numerical simulations

Numerical simulations with COMSOL Multiphysics (COMSOL, Inc., Burlington, MA) were performed to evaluate the accuracy of the CPC-ABC model, and to quantify the effect of the soil-atmosphere interface on HP signals and estimated thermal property values. The Peng et al. (2019) type-HP sensor, with r of 10 mm, was considered in the simulation framework. The probe in the middle of the array served as the heater (H, 2.38-mm o.d. and 0.96-mm i.d.) and the side probe served as the temperature probe (S, 2.00-mm o.d. and 1.5-mm i.d.) (Fig. 1a).

For the numerical simulations, we used a two-dimensional composite rectangle (80 × 80 mm) with zero initial temperature to model the HP system near the soil-atmosphere interface (Fig. 1). We assumed that there was no contact resistance at the material interfaces within this domain. The probes (H and S) of a HP sensor were positioned at (x, z) = (0, 0) and (x, z) = (r_0, 0) in the problem domain (Fig. 1a). The finite thermal conductivity and heat capacity of the heater and temperature probes were considered (Table A1), accounting for the fact that the probes H and S were composite solids that consisted of stainless steel and thermally conductive epoxy. All boundaries except for the soil-atmosphere interface were set as adiabatic boundary conditions (Liu et al., 2013).

Simulations were performed for a hypothetical sand soil (94% sand and 5% clay) with q', t_0, and t values set as 31 W m^{-1}, 25 s, 300 s, respectively, and h varied from 1 mm to 24 mm. For the upper region, the C, κ, and λ inputs were assumed to be equal to those of the air (Table A2). For the lower region, the C, κ, and λ parameters were assumed to be equal to those of soil (Table A2), which were estimated by using thermal property models (i.e., the de Vries (1963) C model and the Lu et al. (2014) λ model) with designated soil texture, θ (from dry to saturation) and bulk density (ρ_b, 1.60 Mg m^{-3}). The values of C and λ within each region of the domain were homogeneous, isotropic, and independent of temperature. In the lower region, the thermal conductivity and heat capacity of heater and temperature probes were also included in the numerical simulations (Fig. 1a). The heat released from the heater was uniformly distributed across the cross-section of the epoxy in the heater probe, and the temperature at the sensing probe in the problem domain satisfied the line-source heat equation. The COMSOL platform was used to generate numerically simulated temperature-by-time curves from the inputs of soil thermal property values and other parameters. Finally, C, κ, and λ were estimated by nonlinearly fitting the CPC-ABC and CPC models to the numerically simulated temperature-by-time curves with a MATLAB program.

2.3. Laboratory HP measurements

Laboratory experiments were also performed on repacked soil samples (94% sand and 5% clay) to obtain temperature-by-time curves by using the HP sensor described by Peng et al. (2019). The sensor has a middle probe (H) and two side probes (S). In this study, we only used the HP measurements at the H probe and one S probe.

To prepare the soil cores, the soil was air-dried, passed through a 2 mm sieve, and packed into cylinders (80 × 80 mm) with the designated θ (0.00 and 0.30 m^3 m^{-3}) and ρ_b values (1.60 Mg m^{-3}). All of the measurements were obtained at a room temperature of 20 ± 1°C, thus the influences of diurnal temperature fluctuations, soil water evaporation, absorbed solar radiation, and convective heat transfer were ignored. Similar to the sensor setup listed in Fig. 1a, the HP sensor was then inserted into each soil column with the sensor plane horizontal to the soil-atmosphere interface with h ranging from 3 mm to 24 mm. A data logger (Model CR3000, Campbell Scientific, Logan, UT) controlled the heat pulse and recorded the temperature-by-time data. Details for analyzing HP data to obtain soil thermal property values were reported by Peng et al. (2019). Soil C, κ, and λ were estimated by fitting the CPC (Eqs. (1), (2) and (6)) and CPC-ABC (Eqs. (1) to (6)) models to the measured temperature-by-time curves. After making the HP measurements, the soil cores were oven dried at 105°C to obtain the actual θ and ρ_b values.

2.4. Error analysis

We assumed that effect of the soil-atmosphere interface was negligible below a soil depth of 24 mm, which was greater than the 2.37r value suggested by Campbell et al. (1991). For the COMSOL simulations, soil thermal property values estimated via the CPC-ABC model were compared to reference values obtained with numerical simulations with a HP sensor at a burial depth of 24 mm. The relative error (RE) was calculated as follows,

$$RE = \frac{x_e - x_i}{x_i} \times 100\% \quad (7)$$

where x_i represents reference soil thermal property values; x_e represents values estimated by the CPC-ABC solution or the CPC solution. For laboratory experiments, a special x_e and x_i term is listed for RE calculations. x_i and x_e denote the CPC-ABC and CPC estimated soil thermal property values, respectively.

3. Results and discussion

3.1. Estimated and simulated HP signals with CPC-ABC model

Fig. 2 shows the CPC-ABC modeled temperature-by-time curves for various HP sensor burial depths and the corresponding simulated values for the hypothetical sand soil at dry and saturation conditions. The values of maximum temperature rise (ΔT_m) and arrival time (t_m) values are determined by soil thermal property values (i.e., C and κ). As expected, the ΔT_m and t_m values decreased with increasing soil θ and h values (Fig. 2). For example, the COMSOL simulated ΔT_m values were 1.14°C for the dry sand (Fig. 2a) and 0.55°C for the water-saturated sand (Fig. 2b), while the t_m values varied from 128 s for the dry sand (Fig. 2a) to 54 s for the water-saturated sand (Fig. 2b). With increasing h values, there was a greater contribution of the soil region to thermal property values within the measurement range, and the simulated ΔT_m values decreased gradually (e.g., 0.98°C at h of 5 mm and 0.69°C at h of 15 mm, Fig. 2a). The CPC-ABC solution modeled temperature-by-time curves matched well with the COMSOL simulated values for both dry and saturated soil conditions.

3.2. Soil thermal property values estimated with the CPC and CPC-ABC models

Fig. 3 shows the REs of the estimated thermal property values derived from the CPC and CPC-ABC models for the dry (a) and water-saturated (b) sand soils at various h values in the simulations. The CPC estimated soil thermal property values at h = 24 mm were set as

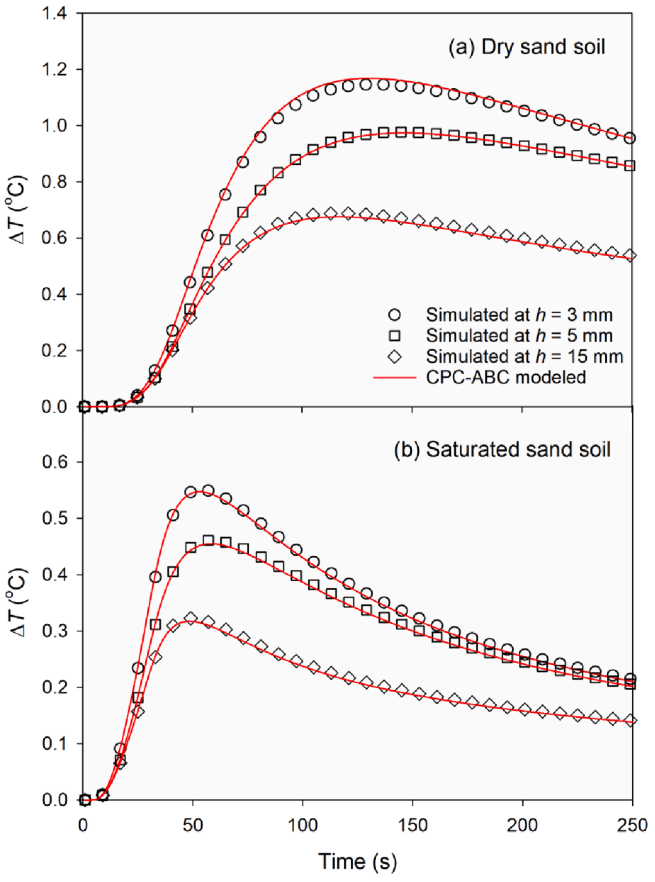

Fig. 2. The CPC-ABC modeled temperature-by-time curves at various burial depths (h) of the HP sensor and the corresponding COMSOL simulated values for the hypothetical sand soil at dry and saturation conditions. The circles, squares and diamonds are numerical simulation results at $h = 3$ mm, 5 mm and 15 mm, respectively. The red lines represent the CPC-ABC modeled temperature-by-time curves at the corresponding depths.

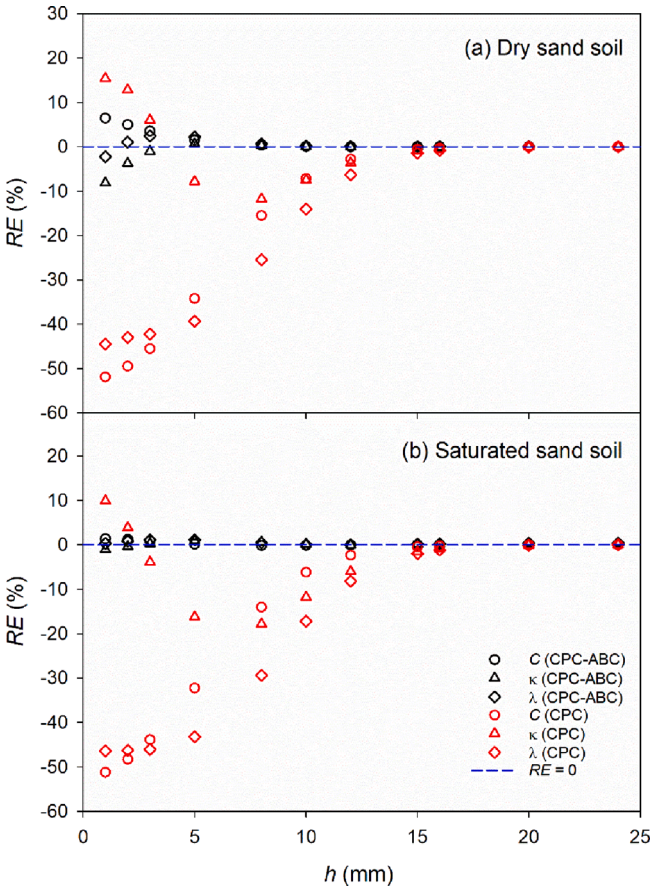

Fig. 3. The relative errors (RE) of soil thermal property values estimated with the CPC-ABC and CPC models for dry (a) and water-saturated (b) samples at various burial depths (h). The black circles, squares and diamonds are CPC-ABC model estimated soil heat capacity (C), thermal diffusivity (κ) and thermal conductivity (λ), respectively. The red circles, squares and diamonds are CPC model estimated soil C, κ and λ values, respectively. The blue dashed line represents a RE value of 0.

reference values to quantify the REs for other scenarios.

As is shown in Fig. 3, the REs of C, κ, and λ decreased for both dry and water-saturated sands as h increased. Thus, errors in C, κ, and λ estimates occurred when the HP sensor was located near the soil-atmosphere interface, but error magnitude decreased as the HP sensor was positioned away from the soil-atmosphere interface. For the CPC model, the REs of soil C, κ, and λ at $h = 1$ mm were 52% for dry sand and 51% for water-saturated sand, but for the CPC-ABC model, the REs of soil C, κ, and λ were less than 8%. The effect of the soil-atmosphere interface on HP measurements was smaller for the wet soil with larger thermal property contrast between air and soil, than that for the dry sand with relatively small C and λ values. As a result, the effect of the soil-atmosphere interface on HP measurements was larger in dry sand than that in water-saturated sand for a given h. Thus, the performance of the CPC-ABC model was saturation dependent (Fig. 3).

For h values greater than 15 mm, the CPC-ABC and CPC derived values for C, κ, and λ of the dry and water saturated samples were generally within 2%, indicating that the probe installation depth should be $>$ 15 mm from the soil-atmosphere interface when using the CPC model to estimate soil thermal property values. The effect of the soil-atmosphere interface also depended on sensor dimensions. Liu et al. (2013) used a HP sensor with 40 mm stainless-steel tubing probe lengths, and showed that the h value should be $>$ 8 mm when the ILS model was used to estimate soil thermal property values of dry sand. Larger probe dimensions, require deeper installation depths to effectively reduce soil-atmosphere interface effect.

The following results were obtained by comparing the estimated HP signals with the CPC-ABC model versus the simulated values on a hypothetical sand soil (48% sand and 14% clay). First, both approaches provided similar results. Secondly, at the burial depth of 1 mm, the REs of the CPC-ABC model were less than 8.4% for both dry and water-saturated samples, which similar close to those obtained on the sand soil (8.2%). Thirdly, when h was greater than 15 mm, the effect of the soil-atmosphere interface could be ignored when the CPC model was applied to estimate soil thermal property values. Thus, the effect of the soil-atmosphere interface on HP measured soil thermal property values depended mainly on the sensor dimension, but were independent of soil texture and water content.

3.3. Experimental evaluation of the CPC and CPC-ABC models

Packed sand column experiments were performed on a sand soil to further verify the effect of the soil-atmosphere interface on HP measurements. We compared the HP measured temperature-by-time curves at various depths and the corresponding CPC-ABC modeled values at θ = 0.00 and 0.30 $m^3\ m^{-3}$(Fig. A1). Results showed that the measured and modeled temperature-by-time curves matched well under both dry and wet conditions. In addition, the ΔT_m and t_m values decreased with increasing soil θ and h values, which corresponded well with the results from the numerical simulations (Fig. A1).

Fig. 4 shows the REs of CPC-C, κ and λ values against the CPC-ABC derived values based on the HP data obtained at various h values in packed sand columns. For both models, errors in the soil thermal

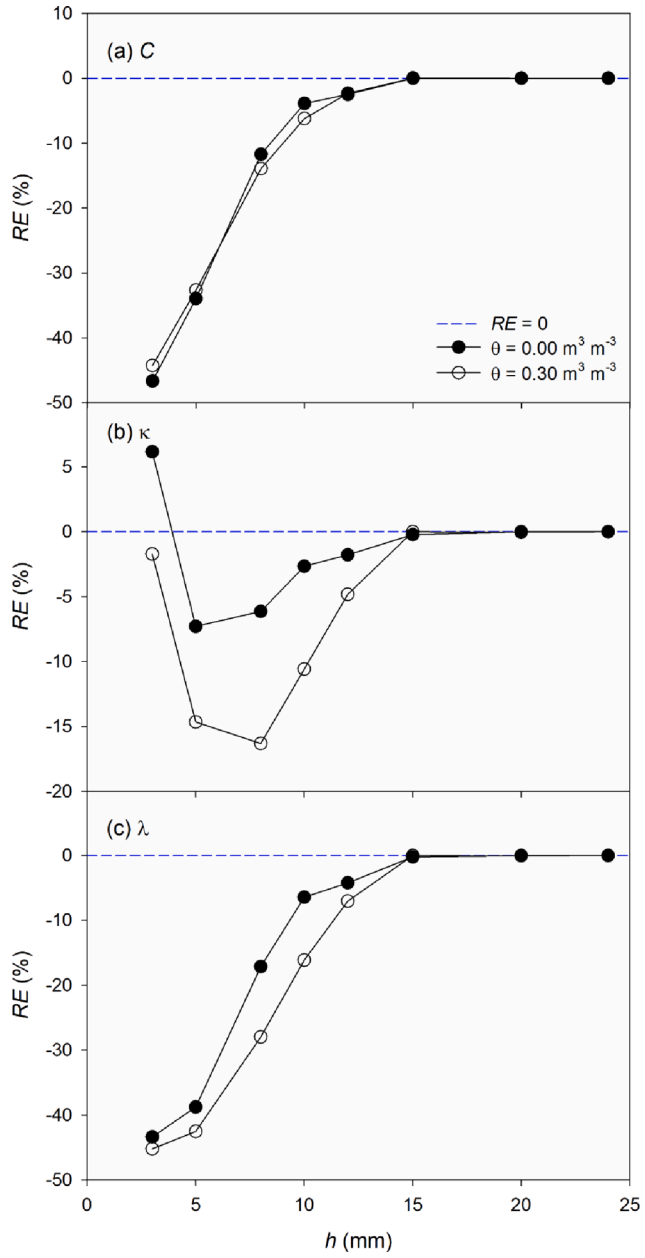

Fig. 4. The relative errors (*RE*) of soil heat capacity (*C*), thermal diffusivity (κ) and thermal conductivity (λ) estimated with the CPC model compared to those estimated with the CPC-ABC model for sand soils with water content (θ) of 0.00 and 0.30 $m^3\ m^{-3}$ at various burial depths (*h*). The blue dashed line represents a *RE* value of 0.

property occurred when the HP sensor was located near the soil-atmosphere interface, and larger errors occurred with smaller *h* values. Compared to *RE*s of the CPC-ABC model, the *RE*s of the CPC-estimated *C*, κ and λ values were −46.7%, 6.2% and −43.4% at *h* of 3 mm. Thus, an overestimation of κ and underestimation of *C* and λ values occurred in the dry sand samples. At *h* of 15 mm, however, the corresponding *RE*s of CPC-estimated *C*, κ and λ values were generally within ± 0.2%. Thus, the CPC model provided accurate *C*, κ and λ values for both dry and wet sand soil samples, which agreed well with the conclusions from the simulation study. At the same *h*, larger errors in *C*, κ, and λ estimates were observed on wet samples as compared with those obtained on dry samples, indicating that the soil-atmosphere interface had a larger effect on the HP results in wet sand soil than in dry sand soil (Fig. 4), which was caused by the fact that the relatively large λ value of wet soil enabled faster heat transfer (Liu et al., 2013).

The burial depth at which the soil-atmosphere interface has a negligible effect on the HP measurements also varies with the sensor dimensions (e.g., the probe diameter and probe-to-probe spacing). Our simulation study indicated that for larger-size sensors, greater burial depths should be used. In this study, the HP sensor has a length of 70 mm, a probe-to-probe spacing of 10 mm, and a diameter of 2.38 mm for the heater probe and 2.0 mm for the temperature probe. If the probe diameter (o.d.) is increased to 4 mm and the probe-to-probe spacing is expanded to 17 mm, a minimum *h* value of 21 mm is required to minimize the effect of the soil-atmosphere interface. Additionally, the CPC-ABC model ignores several environmental factors such as diurnal fluctuations in soil temperature, convective heat transfer, and vapor flow in soils. Further investigations are needed to evaluate the performance of the CPC-ABC model under field conditions.

4. Conclusion

In this study, an extended CPC-ABC solution considering the effects of the soil-atmosphere interface and finite probe properties was introduced to evaluate HP determined soil thermal property values in near-surface soil. The method of images was used to derive the CPC solution with an adiabatic boundary condition. Compared to numerical simulations and laboratory experiments results, the CPC-ABC model accurately depicted simulated and measured HP signals. For burial depths less than 15 mm, ignoring soil-atmosphere interface effect caused errors as large as 50% in soil thermal property estimates associated with the CPC model. However, soil-atmosphere interface effect could be ignored when sensors were horizontally installed at 15 mm or more below the soil surface (i.e., $h > 15$ mm). Further studies should focus on how sensor dimensions, soil types and water conditions affect the performance of the CPC-ABC solution for various application scenarios.

CRediT authorship contribution statement

Wei Peng: Writing – original draft, Data curation. **Yili Lu:** Writing – review & editing. **Tusheng Ren:** Writing – review & editing. **Robert Horton:** Writing – review & editing.

Declaration of competing interest

The authors declare that they have no known competing financial interests or personal relationships that could have appeared to influence the work reported in this paper.

Acknowledgements

This research was supported by the National Natural Science Foundation of China (42307390), Natural Science Foundation of Hebei Province (D2023205026), Technology Innovation Fund from Hebei Normal University (L2023B35), the U.S. National Science Foundation (2037504) and USDA-NIFA Multi-State Project 4188 and 5188.

Appendix A

Table A1
Volumetric heat capacity (C) and thermal conductivity (λ) values for HP sensor probe materials used in this study. These values were estimated with Eq. (42) in Knight et al. (2012).

Parameters	Unit	Value
Heat capacity of heater probe (C_H)	MJ m^{-3} K^{-1}	3.42
Heat capacity of temperature probe (C_S)	MJ m^{-3} K^{-1}	2.56
Soil thermal conductivity of heater probe (λ_H)	W m^{-1} K^{-1}	12.64
Soil thermal conductivity of temperature probe (λ_S)	W m^{-1} K^{-1}	7.10

Table A2
Volumetric heat capacity (C), thermal diffusivity (κ) and thermal conductivity (λ) values for the sand soil used in the numerical simulations. Soil C values were estimated with the de Vries (1963) C model, and soil λ values were estimated with the Lu et al. (2014) λ model. Soil κ was estimated by dividing λ by C.

Materials	C MJ m^{-3} K^{-1}	κ 10^{-7} m^2 s^{-1}	λ W m^{-1} K^{-1}
Air[+]	0.0012	214	0.0257
Dry sample	1.26	2.78	0.35
Sample at θ of 0.10 m^3 m^{-3}	1.68	7.98	1.34
Sample at θ of 0.20 m^3 m^{-3}	2.10	8.24	1.73
Saturated sample	2.79	7.49	2.09

[+]data from Montgomery (1947).

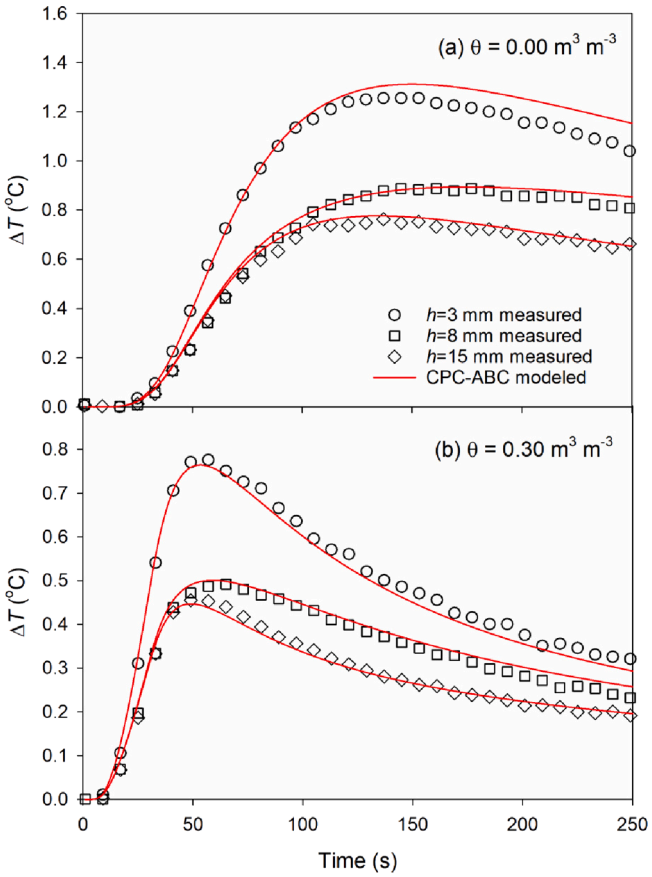

Fig. A1. The HP measured temperature-by-time curves at various burial depths (h) of the HP sensor and the corresponding CPC-ABC modeled values for the sand soils at water content (θ) of 0.00 and 0.30 m^3 m^{-3}. The circles, squares and diamonds are measured results at h = 3 mm, 8 mm and 15 mm, respectively. The red lines represent the CPC-ABC modeled temperature-by-time curves at the corresponding depths.

References

Campbell, G.S., Calissendorff, K., Williams, J.H., 1991. Probe for measuring soil specific heat using a heat-pulse method. Soil Sci. Soc. Am. J. 55, 291–293.
Carslaw, H.S., Jaeger, J.C., 1959. Conduction of heat in solid. Clarendon Press, Oxford.
de Vries, D.A., 1963. Thermal properties of soils. In: Van Wijk, W.R. (Ed.), Physics of Plant Environment. North-Holland Publ, Amsterdam, pp. 210–235.
He, H.L., Dyck, M.F., Horton, R., Ren, T.S., Bristow, K.L., Lv, J., Si, B.C., 2018. Development and application of the heat pulse method for soil physical measurements. Rev. Geophys. 56, 567–620.

Heitman, J.L., Xiao, X., Horton, R., Sauer, T.J., 2008. Sensible heat measurements indicating depth and magnitude of subsurface soil water evaporation. Water Resour. Res. 44, W00D05.
Kamai, T., Kluitenberg, G.J., Hopmans, J.W., 2015. A dual-probe heat-pulse sensor with rigid probes for improved soil water content measurement. Soil Sci. Soc. Am. J. 79, 1059–1072.
Kluitenberg, G.J., Knight, J.H., Kamai, T., 2021. Integral form of the cylindrical perfect conductors solution for the dual-probe heat-pulse method. Soil Sci. Soc. Am. J. 85, 1963–1969.
Knight, J.H., Kluitenberg, G.J., Kamai, T., Hopmans, J.W., 2012. Semianalytical solution for dual-probe heat-pulse applications that accounts for probe radius and heat capacity. Vadose Zone J. 11.
Liu, G., Zhao, L.J., Wen, M.M., Chang, X.P., Hu, K.L., 2013. An adiabatic boundary condition solution for improved accuracy of heat-pulse measurement analysis near the soil–atmosphere interface. Soil Sci. Soc. Am. J. 77, 422–426.
Lu, Y.L., Lu, S., Horton, R., Ren, T.S., 2014. An empirical model for estimating soil thermal conductivity from texture, water content, and bulk density. Soil Sci. Soc. Am. J. 78, 1859–1868.
Montgomery, R.B., 1947. Viscosity and thermal conductivity of air and diffusivity of water vapor in air. J. Meteorolog. Res. 4, 193–196.
Peng, W., Lu, Y.L., Xie, X.T., Ren, T.S., Horton, R., 2019. An improved thermo-TDR technique for monitoring soil thermal properties, water content, bulk density, and porosity. Vadose Zone J. 18, 190026.
Peng, W., Lu, Y.L., Ren, T.S., Horton, R., 2021. Application of infinite line source and cylindrical-perfect-conductor theories to heat pulse measurements with large sensors. Soil Sci. Soc. Am. J. 85, 1050–1059.
Peng, W., Lu, Y.L., Ren, T.S., Horton, R., 2022. Analysis of heat pulse measurements in double-layered soils with the heating probe positioned at the layer interface. Geoderma 424, 115987.
Philip, J.R., Kluitenberg, G.J., 1999. Errors of dual probes due to soil heterogeneity across a plane interface. Soil Sci. Soc. Am. J. 63, 1579–1585.
Stehfest, H., 1970a. Algorithm 368: Numerical inversion of Laplace transforms. Commun. ACM 13, 47–49.
Stehfest, H., 1970b. Remark on Algorithm 368: Numerical inversion of Laplace transforms. Commun. ACM 13, 624.
Xiao, X., Horton, R., Sauer, T.J., Heitman, J.L., Ren, T.S., 2014. Sensible heat balance measurements of soil water evaporation beneath a maize canopy. Soil Sci. Soc. Am. J. 78, 361–368.
Xiao, X.H., Zhang, X., Ren, T.S., Horton, R., Heitman, J.L., 2015. Thermal property measurement errors with heat-pulse sensors positioned near a soil-air interface. Soil Sci. Soc. Am. J. 79, 766–771.
Zhang, X., Lu, S., Heitman, J., Horton, R., Ren, T.S., 2012. Measuring subsurface soil-water evaporation with an improved heat-pulse probe. Soil Sci. Soc. Am. J. 76, 876–879.
Zhang, X., Heitman, J.L., Horton, R., Ren, T.S., 2014. Measuring near-surface soil thermal properties with the heat-pulse method: Correction of ambient temperature and soil-air interface effects. Soil Sci. Soc. Am. J. 78, 1575–1583.